

BEAM PROFILE REFLECTOMETRY: A NEW TECHNIQUE FOR THIN FILM MEASUREMENTS

J.T. Fanton, Jon Opsal, D.L. Willenborg,
S.M. Kelso, and Allan Rosencwaig
Therma-Wave, Inc.
Fremont, CA 94539

INTRODUCTION

In the manufacture of semiconductor devices, it is of critical importance to know the thickness and material properties of various dielectric and semiconducting thin films. Although there are many techniques for measuring these films, the most commonly used are reflection spectrophotometry [1,2] and ellipsometry [3]. In the former method, the normal-incidence reflectivity is measured as a function of wavelength. The shape of the reflectivity spectrum is then analyzed using the Fresnel equations to determine the thickness of the film. In some cases, the refractive index can also be determined provided that the dispersion of the optical constants are well known. The latter method consists of reflecting a beam of known polarization off the sample surface at an oblique angle. The film thickness, and in some cases the refractive index, can be determined from the change in polarization experienced upon reflection.

While these two methods have adequately addressed the needs of the semiconductor industry in the past, limitations in both of these technologies present serious challenges to some of the more demanding measurement requirements of the industry today. For example, there are a great variety of materials being used, such as chemical vapor deposition (CVD) oxides, nitrides and oxynitrides, polysilicon and amorphous silicon, and metals, whose optical properties depend on the actual deposition conditions. To determine the thickness accurately, it is often necessary to measure the refractive index, n , or even the extinction coefficient, k , as well. The need to know the dispersion of these optical constants limits the ability of the spectroscopic methods to perform multiparameter measurements. The ellipsometric methods are limited by cyclical ambiguities and dead zones in the measurements of films thicker than a half-wavelength of the light.

Additionally, to perform measurements in the small geometries of product wafers the measurement spot should be as small as possible. The oblique angle of incidence used in ellipsometers limits their spot sizes to about $25\mu\text{m}$; spectrophotometers are limited to about $3\text{--}4\mu\text{m}$ due to available light budgets. Ideally, the industry would prefer a sub-micron spot.

PRINCIPLE OF BEAM PROFILE REFLECTOMETRY

The beam profile reflectometer (BPR) is a new approach that measures the reflectivity of the sample for a fixed wavelength as a function of angle of incidence. It is an adaptation of a

much older technique called variable angle reflectometry [4-6] (VAR) but unlike VAR, the BPR measures all of the angular reflectivities *simultaneously*. This is accomplished by analyzing the intensity profile of a highly focussed beam. A collimated laser beam focussed through a 0.9 NA microscope objective, for example, converges upon the sample surface at angles ranging continuously from 0° to 64°.

As shown in Fig. 1a, there is a one-to-one correspondence between the radial position of the beam entering the lens, and the subsequent angle of incidence upon the sample. Since the interference through the film stack changes with angle, the reflected light experiences an angular variation in reflectivity which, in turn, gives rise to a positional variation in the intensity of the reflected collimated beam. The resulting beam profile consists of a series of concentric fringes that is characteristic of the particular film being studied.

In addition, if the input beam is linearly polarized, the polarization of the light incident upon the sample will also have a positional dependence (see Fig. 1b). In particular, light passing through the diameter of the lens oriented along the direction of input polarization will be purely P-polarized when it strikes the sample. Likewise, light travelling through the orthogonal diameter will be purely S-polarized. Thus the P- and S-polarization responses of the film can be measured simultaneously from 0° to 64° by analyzing the reflected intensity profiles of the light that passes through these two regions of the lens.

Of course, using a high NA microscope objective not only provides a wide range of angular information, it also results in a very small measurement spot. Since the diffraction-limited spot size is roughly λ/NA , the measurement area is sub-micron for any visible wavelength.

THE INSTRUMENT

A schematic of the beam profile reflectometer is shown in Fig. 2. The angular reflectivity measurements are made using light from a linearly polarized 675 nm wavelength diode laser. The light is focussed to a sub-micron spot with a 0.9 NA microscope objective whose focal distance is precisely maintained by a piezoelectrically driven autofocus system. Adjacent to the objective lens is the incident-power detector. To minimize noise caused by laser power fluctuations, all signals are normalized by the measured laser output power.

The reflected beam is divided by a series of 50/50 beamsplitters and sent to a total of four detectors. Two of the detectors are linear CCD arrays oriented along the lines of pure S- and pure P-polarization. These arrays measure the intensity at 256 points across the beam thus providing the S and P signatures of the film. Note that the light intensity hitting these arrays depends not only on the reflectivity but on the original power distribution across the beam emerging from the laser. In order to determine the reflectivity, the measured signals are divided by a stored profile of a bare-silicon reference.

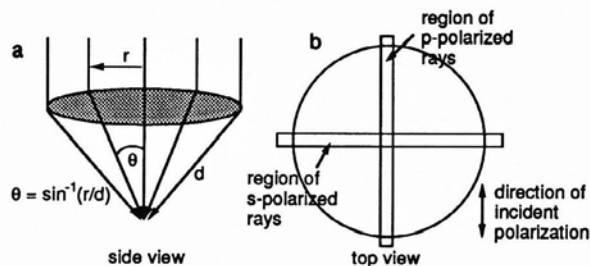


Fig. 1. (a) Relationship between radial position and angle of incidence. (b) Regions of the lens where pure s or p polarization is preserved.

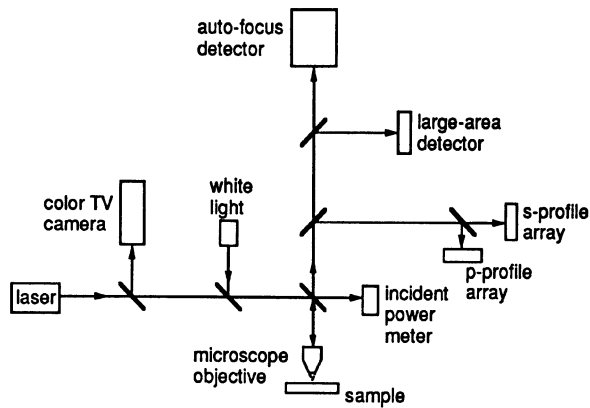


Fig. 2. Schematic of the beam profile reflectometer.

We use silicon as the reference material for two reasons. First, the surface quality and optical uniformity of readily available material is outstanding. Second, since this material normally has only a very thin ($\sim 20\text{\AA}$) layer of native oxide, its reflectivity is essentially insensitive to any further changes (or growth) in the surface film.

A third detector measures the total reflected power in the entire beam. This detector measures, in essence, the integrated signal from all the rays (P-, S-, and P + S-polarized). Although the signal from this detector contains no more information than the arrays, it is possible to obtain better signal-to-noise in a single-cell detector that measures the entire beam. This is useful in situations where extreme precision is required, such as when measuring films thinner than 100\AA .

The fourth detector senses the reflected laser collimation to drive a focus servo system. The autofocus servo has a vertical positioning resolution of 10 nm and a bandwidth of greater than 100 Hz.

In addition to the laser path, there is a white light path which is used for viewing the sample on a color TV monitor. The camera image is also used in a pattern-recognition system for automatic measurements on patterned wafers.

FILM ANALYSIS

As mentioned above, there is a direct correspondence between the radial position in the collimated input laser beam and the subsequent angle of incidence upon the sample. Thus the intensity pattern of the reflected collimated beam will depend upon the angular reflectivity characteristics of the film stack being measured. The theoretical reflectivity of a stack can be found by piecing together the reflections from the individual layers. For a film with m interfaces (see Fig. 3), the S and P reflectivities at the last (m^{th}) interface are given by the well known Fresnel coefficients [7]:

$$r_{sm} = \frac{\sin(\theta_{m+1} - \theta_m)}{\sin(\theta_{m+1} + \theta_m)} \quad (1)$$

$$r_{pm} = -\frac{\tan(\theta_{m+1} - \theta_m)}{\tan(\theta_{m+1} + \theta_m)} \quad (2)$$

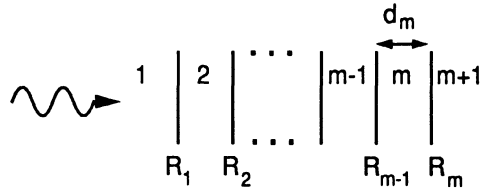


Fig. 3. Diagram of the film stack used in the analysis of the reflectivity.

where r_{sm} and r_{pm} are the respective reflectivities for S- and P-polarized light. The propagation angle, θ_m , is related to the primary angle of incidence in the air, θ_{air} , through Snell's Law, $n_m \sin\theta_m = \sin\theta_{air}$ where n_m is the refractive index of the material.

For simplicity, we can drop reference to the polarization and denote the reflectivity from the m^{th} interface as R_m . Working back to the preceding interface, the round-trip phase lag is given by $2k_{zm}d_m$ where k_{zm} is the z-component of the propagation constant, given by

$$k_{zm} = 2\pi/\lambda_0 \sqrt{n_m^2 - \sin^2\theta_{air}}, \quad (3)$$

and d_m is the thickness of the layer. We can then invoke continuity of the transverse electric and magnetic fields to derive the total reflectivity of the bottom two materials:

$$R_{m-1} = \frac{r_{m-1} + R_m e^{i2k_{zm}d_m}}{1 + r_{m-1}R_m e^{i2k_{zm}d_m}} \quad (4)$$

This formula is recursive and can be iterated up to the top layer to find the reflectivity of the entire film stack. Absorbing films are accommodated by making the refractive index complex.

We can get an idea of the information available in a typical measurement by examining the profiles for a simple, single-layer film. Fig. 4 shows the theoretical S and P profiles for a 1 μm oxide film on a silicon substrate. Recall that these profiles have been normalized by profiles of the reference material; the plots thus represent the reflectivity of the sample relative to that of bare silicon. Note that the peaks of the curves reach a value of 1. These peaks are located at angles where half-wave interference occurs; ie. when $k_z d = \pi$. The amplitude at the peaks is independent of the film thickness or film index; it is determined entirely by the substrate index. Thus, for this profile we see that the substrate has the same index as our reference material.

At the other extreme, the minima in the curves occur very nearly at the quarter-wave matching condition, especially in the s-profile. (The strong angular variation of the p-reflectivity on bare silicon tends to shift the normalized p-profile minimum.) Here the level is again roughly independent of the film thickness; the reflectivity is a function of only the two refractive indices and the angle of incidence. Since the substrate index can be determined from the peaks, the minima can be used to find the film index.

Finally, the p-profile provides its own verification of the film index through its behavior near Brewster's angle for the air-SiO₂ interface. At Brewster's angle, there is no reflection from the top surface; the reflectivity is just that of the substrate alone. Thus the location of Brewster's angle (in this case, the angle at which the normalized profile equals 1) determines the film index through the relation $\tan\theta_B = n$.

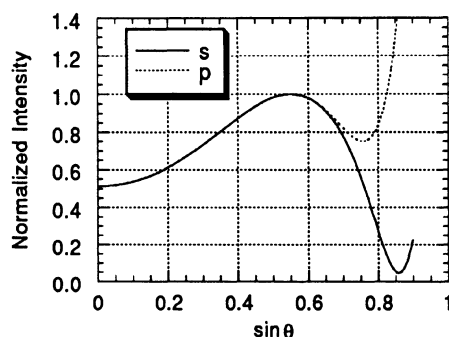


Fig. 4. Theoretical s and p profiles for a $1\ \mu\text{m}$ SiO_2 film on a silicon substrate.

Having determined the film and substrate indices, the film thickness is then given by the angular location of the maxima and minima or, more generally, from the stretch of the curve. For thicker films, there are more cycles in the profiles.

In practice, we do not explicitly examine specific features of the profiles when analyzing a film stack. Instead, the unknown film parameters are determined from a least-squares fit to the measured data using Eqs. (3) and (4). Our ability to determine more than one thickness or optical constant is a natural result of the independent influences these parameters have upon the shapes and magnitudes of the two profiles.

MEASUREMENT RESULTS

Here we present a few examples that demonstrate the multi-parameter fitting capabilities of the BPR. In many of these situations, the ability to measure more than one parameter was not only convenient but essential for obtaining the proper solution. Frequently, errors in specifying "known" quantities lead to erroneous measurements.

The first example is a two-layer stack of amorphous silicon ($\alpha\text{-Si}$) on oxide. This is included to show the accuracy of multi-parameter fitting. The intended film stack was an 8000\AA $\alpha\text{-Si}$ layer over 1000\AA of oxide. We used the BPR to measure the thickness of both layers as well as the extinction coefficient of the $\alpha\text{-Si}$. We originally tried measuring the refractive index of the $\alpha\text{-Si}$ as well, but we stopped when we discovered it was coming out lower than it should for this material. Therefore, we used our standard index in the thickness measurements and found that the films measured 7260\AA over 880\AA . A subsequent TEM, Fig. 5, showed values of 7100\AA and 880\AA , thereby confirming our measurements. The source of the slight discrepancy in $\alpha\text{-Si}$ readings was also discovered: about 1000\AA of the amorphous silicon has crystallized to form polysilicon (note the large grains near the $\alpha\text{-Si} - \text{SiO}_2$ interface). Since the refractive index of this material is about 10% lower than $\alpha\text{-Si}$, it is no surprise that our index measurements were coming out lower than we expected. Furthermore, the effect of this additional layer upon the reflectivity is sufficient to account for the 0.2% thickness error.

Another example demonstrates the ability of the BPR to perform accurate multiparameter film measurements without influence from varying substrate conditions. The instrument was used to measure the thickness and index of two similar silicon nitride films. However, in the first sample the film was deposited on bare silicon while in the second, a 350\AA oxide layer was grown on the silicon prior to the nitride deposition. The nitride depositions were done in the same run so similar thicknesses were expected. For the simple nitride we measured both the film thickness and index, while for the nitride/oxide sample we measured the oxide thickness as well. As seen in the area maps shown in Fig. 6, the BPR found the same

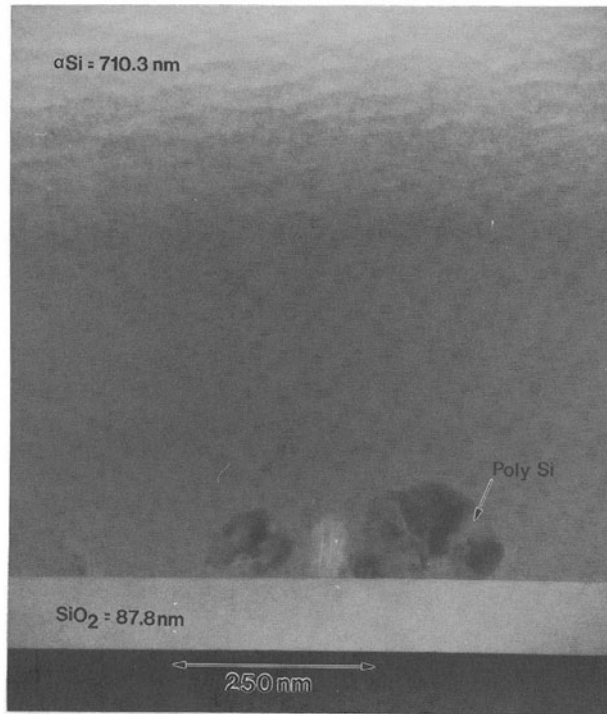


Fig. 5. Transverse electron micrograph of amorphous silicon / SiO₂ film stack.

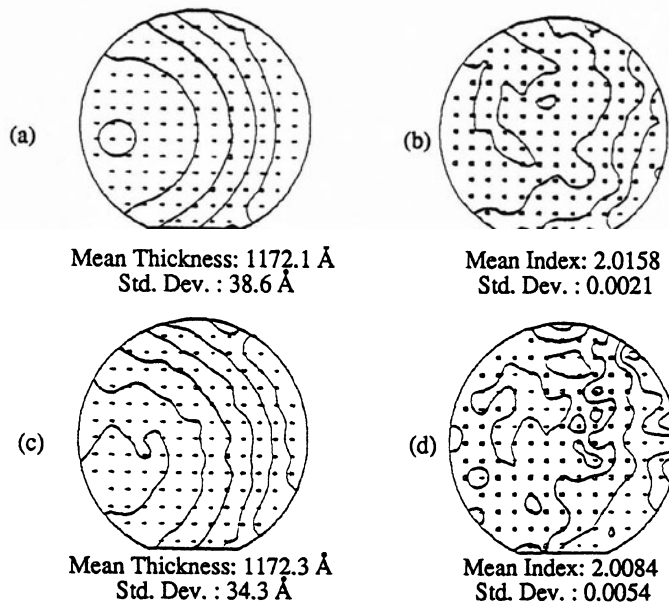


Fig. 6. Area maps of measured thickness and index of a Si₃N₄ film. Figs. 6a and 6b show the results for a simple silicon substrate; Figs. 6c and 6d show the results for a substrate of 350 Å of oxide over silicon.

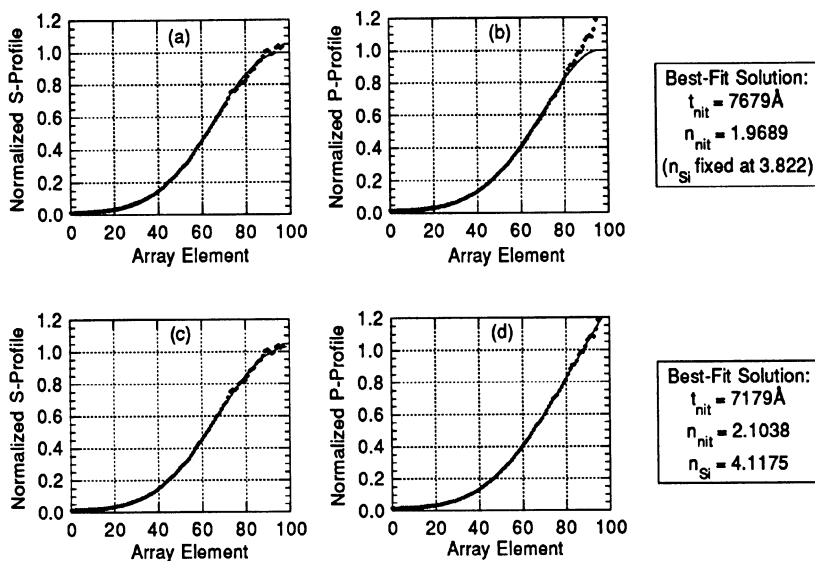


Fig. 7. Measurements (points) and best-fit solution (solid curve) for a PECVD nitride film on silicon. Figs. 7a and 7b show the best fit assuming a normal silicon substrate. Figs. 7c and 7d show the fit when the substrate index is measured as well.

thickness and index for the two nitride films. Neither the presence of the oxide, nor the inclusion of a third fitting parameter deterred from the accuracy of the measurement.

Although the ability to measure many parameters simultaneously can be convenient, it is sometimes also necessary even if only one parameter is of real interest. For example, Fig. 7 shows the measured profile and calculated thickness and index of a PECVD nitride film deposited on silicon. Note how the profiles exceed 1 at their maxima; clearly, the substrate cannot be simple silicon. If we include the substrate index in our list of unknown parameters the fits improve dramatically and, most importantly, the film thickness and index measurements (listed to the right of the plots) change significantly. The increase in substrate index is due to damage caused by the plasma enhanced process. We typically see this effect in PECVD films and we have determined that it is essential to know the substrate index if accurate film measurements are to be performed.

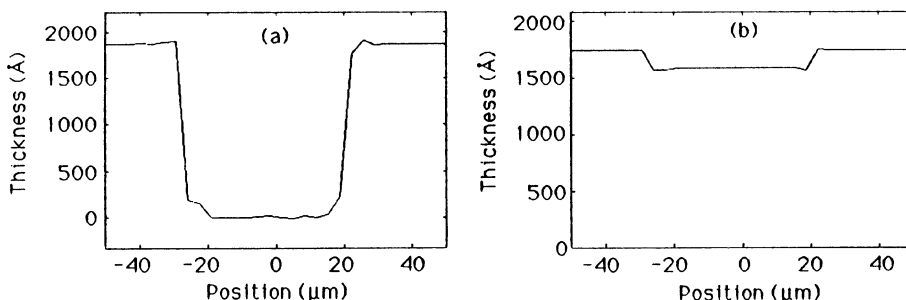


Fig. 8. Simultaneous thickness measurements of the top oxide (a) and the underlying polysilicon (b) in an etched oxide/polysilicon/oxide/Si film stack.

Our final example demonstrates the usefulness of the small measurement spot. The two plots in Fig. 8 are from an oxide/polysilicon/oxide/Si film stack. A 40 μm scribe line was etched in the top oxide down to the polysilicon layer below. By measuring the thickness of the top two layers we were able to show that the poly had suffered about 100 \AA of etching as well. Thus we were able to measure the selectivity of the oxide etch without needing to strip the top oxide as is commonly done.

CONCLUSION

The wealth of information present in the intensity profile of a highly focussed, linearly polarized beam makes the BPR a powerful film measurement technique. The shape and amplitude information in the S and P profiles of angular reflectivity enable us to determine not only the thickness of a simple film, but also the refractive index, extinction coefficient, or even the thicknesses of other films in a multi-layer stack. In some cases, we can measure three or even four different parameters simultaneously. Furthermore, these measurements all occur in a submicron area making possible measurements on product wafers.

REFERENCES

1. O.S. Heavens, *Optical Properties of Thin Solid Films* (Butterworths, London, 1955).
2. F. Reizmann and W. Van Gelder, *Solid-State Electron.* **10**, 625 (1967).
3. R.M.A. Azzam and N.M. Bashara, *Ellipsometry and Polarized Light* (North-Holland, New York, 1979).
4. W.A. Pliskin and E.E. Conrad, *IBM J. Res. Dev.* **8**, 43 (1964).
5. W.A. Pliskin, in *Progress in Analytic Chemistry*, edited by E.M. Murt and W.G. Guedner (Plenum, New York, 1969), Vol. 2, p. 1.
6. T. Kihara and K. Yokomori, *Appl. Opt.* **29**, 5069 (1990).
7. F.A. Jenkins and H.E. White, *Fundamentals of Optics* (McGraw-Hill, New York, 1976).